Reduction Kinetics of Nitroaromatic Compounds by Titanium-Substituted Magnetite

Rémi Marsac [a,#], Mathieu Pasturel [b], Khalil Hanna [*a]

[a]École Nationale Supérieure de Chimie de Rennes, UMR CNRS 6226, 11 Allée de Beaulieu, 35708 Rennes Cedex 7, France

[b]Institut des Sciences Chimiques de Rennes, UMR CNRS 6226, 263 avenue Général Leclerc, 35042 Rennes Cedex 7, France

*Corresponding author: Tel.: +33 2 23 23 80 27; fax: +33 2 23 23 81 20.

E-mail address: khalil.hanna@ensc-rennes.fr (K. Hanna)

[#]Present address: Géosciences Rennes, UMR CNRS 6118, Université de Rennes 1, Campus de Beaulieu, CS74205, 35042 Rennes Cedex, France

Revised manuscript submitted to the *Journal of Physical Chemistry C*

May 2017

Abstract

Although there is a growing interest in environmentally friendly catalytic processes based on magnetic solids, the reactivity of titanomagnetite ($Fe_{3-x}Ti_xO_4$) having a "tunable" solid-state Fe(II)/Fe(III) ratio for reductive transformation of nitroaromatic compounds has been never investigated. This study, for the first time, comprehensively examines the reduction kinetics of nitroaromatic compounds by titanium-substituted magnetite and compares with that of Fe(II) amended-un-substituted magnetite at equal amounts of total Fe(II). Firstly, we have demonstrated that Ti substitution in magnetite increased considerably the ability of magnetite to reduce 4-Nitrophenol (4-NP) as well as Nitrobenzene (NB) in a surface-mediated electron transfer pathway. However, Fe(II)-amendment of magnetite (x=0) to have equivalent amount of total Fe(II) as in the corresponding titanomagnetite ($0.25 \leq x \leq 0.75$) resulted in higher reduction rate constants for both substrates (4-NP and NB). Initial k_{obs} was shown to increase exponentially with $(Fe(II)/Fe(III))_{bound}$ in magnetite, while for titanomagnetites a logarithmic dependence of k_{obs} with increasing $(Fe(II)/Fe(III))_{bound}$ was observed. Only the early stage kinetic behavior differs between titanomagnetite and Fe(II)-amended magnetite at the same total Fe(II) amount. Changes in Fe^{2+}/Fe^{3+} electron delocalization properties or electron hopping, presumably due to the mixing of Fe^{2+} and Ti^{4+} on the octahedral sites, may affect the surface-mediated electron transfer between the solid state and redox sensitive species in solution. These bulk-controlled mechanisms drive the electron transfer process both within the solid phase and across the solid/water interface, thereby altering the regeneration of active sites and ongoing reduction reaction on the magnetite surface.

Introduction

Magnetite is a common mineral that may be formed by biogenic or chemogenic processes in a variety of natural settings. Magnetite can be an important reductant in natural soils, which has been shown to reduce 4-chloronitrobenzene,[1] nitrobenzene,[2-4] carbon tetrachloride[5,6] and other organic contaminants.[7] The stoichiometry of the particles (*i.e.* Fe(II)/Fe(III) ratio that can vary from 0 to 0.5) is one of the most important factors in the reduction reaction, and could govern the reactivity of magnetite in natural and engineered systems.[3,8] Perfectly stoichiometric magnetite particles (i.e. Fe(II)/Fe(III) ratio= 0.5) is the most reactive magnetite, while partially oxidized magnetite or non-stoichiometric magnetite (i.e. low Fe(II)/Fe(III) ratio) loses its reductive effectiveness.[4] Exposing non-stoichiometric magnetite to a source of Fe(II) can restore the 0.5 ratio through oxidation of adsorbed Fe(II), accompanied by reduction of the octahedral Fe(III) in the underlying magnetite to octahedral Fe(II).[3] Since it is generally accepted that the structural Fe(II) is the driving factor in magnetite-mediated reduction, investigations to recharge magnetite surfaces by Fe(II) in order to trigger or enhance the reactivity have attracted great attention.[2,3,7]

Another way to increase the solid state Fe(II)/Fe(III) ratio and then the reductive ability of magnetite is the structural incorporation of elements such as tetravalent titanium (Ti(IV)). For instance, the substitution of Fe(III) by Ti(IV) is accompanied by the reduction of lattice Fe(III) to Fe(II) for charge balance, and thus increases the amount of structural Fe(II) in the inverse spinel structure of magnetite. This spinel ferrite called titanomagnetite ($Fe_{3-x}Ti_xO_4$) was presented as a "tunable" solid-state Fe(II)/Fe(III) redox system,[9-18] and might be seen as advantageous over Fe(II)-recharge of magnetite. The reductive ability of titanomagnetite has been recently investigated, but only for inorganic compounds, *e.g.* Tc(VII), Np(IV) and U(VI).[11,13,14] In these

studies, titanomagnetites are found, as expected, stronger reductants than stoichiometric magnetite due to their higher Fe(II) content, but none of these studies have attempted to compare the reactivity of titanomagnetite with that of Fe(II)-amended magnetite at the same total amount of Fe(II). As the Fe(II)-bearing catalysts are widely used for reductive transformation of nitroaromatic or halogenated compounds,[1-7] the reductive abilities of titanomagnetite and Fe(II)-amended magnetite merit investigation from both environmental and engineering points of view.

The main objective of this study is, therefore, to compare the redox activity of titanomagnetite with that of Fe(II) amended-magnetite at equal amounts of initial Fe(II). For this purpose, titanomagnetites were synthesized with controlled Ti content (x = 0, 0.25, 0.38, 0.5 and 0.75) to tune the solid-state Fe(II)/Fe(III) ratio, and then characterized by transmission electron microscopy (TEM), BET specific surface area analysis, and X-ray diffraction (XRD). 4-nitrophenol (4-NP) was selected as a target contaminant because nitrophenols are one of the most used chemicals in production of dyes, pesticides, and pharmaceuticals and are suspected carcinogens. In addition, conversion of 4-NP to Aminophenol (4-AP) has great commercial relevance because 4-AP is an important intermediate for production of analgesic/antipyretic drugs and acetaminophen (e.g. paracetamol). Nitrobenzene (NB) (a non-phenolic analog to 4-NP), that is widely used as a probe in reduction studies, was also used in order to test the influence of molecular structure on the reductive ability of titanomagnetite. The effect of Ti content (x) and solid loading on variations of kinetic rates and dissolved Fe(II) was investigated. As pH is a key reaction parameter in surface-mediated processes involving Fe species, reduction kinetics by $Fe_{3-x}Ti_xO_4$ and Fe(II)-amended magnetite were determined under anaerobic conditions as a function of pH (6 to 9). The electron transfer processes both within the bulk phase and across the oxide/water interface are discussed in order to explain the discrepancy of reduction kinetics between titanomagnetite and Fe(II)-amended magnetite.

Experimental procedures

Materials. If not mentioned, chemicals (all pro analytical quality or better) were obtained from Sigma Aldrich. Solutions were prepared with ultrapure "MilliQ" water (specific resistivity, 18.2 MΩ cm^{-1}). Magnetite (Fe_3O_4; hereafter denoted "M") and titanomagnetites ($Fe_{3-x}Ti_xO_4$; x = 0.25, 0.38, 0.5 and 0.75; hereafter denoted "TiM0.25", "TiM0.38", "TiM0.5" and "TiM0.75", respectively) were synthesized applying the same procedure, according to the protocol of Pearce *et al.*[10], which involves a room temperature aqueous precipitation method in an anaerobic chamber (JACOMEX; N_2-glovebox; $O_{2(g)}$ < 10 ppm). A 0.3 M HCl solution containing (1 + x) mol L^{-1} $FeCl_2$ and (2 - 2x) mol L^{-1} $FeCl_3$ was prepared first, followed by a dropwise addition of x mol L^{-1} $TiCl_4$. Then, this solution was introduced into an N_2-sparged 25% w/v ammonium (NH_4OH) solution, with continuous stirring at 1400 rpm, leading to instantaneous precipitation of titanomagnetite nanoparticles according to the equation:

$$(1 + x)\ Fe^{2+} + (2 - 2x)\ Fe^{3+} + x\ Ti^{4+} + 8\ OH^- \rightarrow Fe_{3-x}Ti_xO_4 + 4\ H_2O$$

The solids were washed three times with ultrapure water purged with N_2 for 4 h and then centrifuging for 5 min at 4000 rpm. Finally, mother suspensions were prepared by re-suspending titanomagnetite nanoparticles in ultrapure water, which naturally equilibrated at 8 < pH < 8.5.

Characterization of titanomagnetite nanoparticles. An aliquot of each titanomagnetite suspension was taken and digested in N_2-sparged 5 M HCl inside the glovebox overnight with shaking. Dissolved Fe(II) and Fe(III) concentrations were determined applying the phenanthroline method.[19] It was previously shown that chemical analysis could determine accurately Fe(II)/Fe(III) in both magnetite and titanomagnetite.[3,10] The total Fe(II)/Fe(III) ratio of

the samples, as determined by chemical analysis, were expectedly somewhat lower than the theoretical Fe(II)/Fe(III) ratio (Table 1) calculated from the ratio of $FeCl_2/FeCl_3$ used in the synthesis. This results from the washing step employed to remove any unreacted metal chlorides after synthesis,[10] as previously seen for magnetite, which is due to larger dissolution of Fe(II) than Fe(III).[4] Small amounts of titanomagnetite nanoparticles were dried for B.E.T. surface area determination (Tristar, Micromeritics). Surface area is given for each solid in Table 1.

Powder X-ray diffraction (XRD; Bruker D8 Advance diffractometer) analysis was conducted. The diffractometer works with a monochromatized Cu Kα1 radiation (λ = 1.5406 Å) and is equipped with a LynxEye fast detector enabling a photon energy selection and thus the removal of Fe-fluorescence background signal. Titanomagnetite suspension was placed on a misoriented Si single crystal holder and dried for 2 h in an anaerobic chamber. To avoid the oxidation of titanomagnetite during the analysis of XRD, the dried sample was covered with a drop of glycerol. The samples were scanned in the 2θ range from 10° to 130° with steps of 0.01° and integration time of 716 s $step^{-1}$. The XRD patterns of magnetite and of titanomagnetites are indexed with the peaks of magnetite (Fig. S1). Refinement of the XRD patterns using the Le Bail method with the help of the Fullprof software[20] enabled to determine (i) the cell parameters of the phase and (ii) the average crystallite size by fitting the lorentzian enlargement of the peaks compared to a reference corundum sample and deconvoluting the instrumental contribution from the total FWHM using a Thompson-Cox-Hastings profile function (Table 1). The refined cell parameter varies from a = 8.384(2) Å for the unsubstituted magnetite to a = 8.413(2) Å for $Fe_{2.25}Ti_{0.75}O_4$. These values are slightly smaller than the ones reported by Pearce et al.[10] but the difference along the solid solution is identical (0.029 Å) in both cases ($0 \leq x \leq 0.75$ in the present case, $0 \leq x \leq 0.67$ in Pearce et al.[10]). The determined crystallite sizes are 9-13 nm for $0 \leq x \leq 0.5$,

as previously shown.[10-12] For x = 0.75, larger crystallite diameter (28 nm) but larger surface area were found, which might be explained by the inhomogeneous distribution of particles, and the presence of non-structural Ti(IV)/Fe(II) amorphous phase. This amorphous phase appears on the XRD patterns of TiM0.5 and TiM0.75 as very broad diffraction features centered around 34 and 63° (Fig. S1).

Transmission electron microscopy (TEM; Jeol JEM 1230 microscope) was used for titanomagnetite nanoparticles characterization. A small aliquot of titanomagnetite mother suspension was diluted with ethanol solution. A droplet of the diluted suspension was deposited on gold TEM grids and the samples analyzed at an acceleration voltage of 200 kV. TEM images generally revealed aggregates of 10-15 nm diameter sized particles (Fig. S2), but for x = 0.75 larger particles (up to ~50 nm) were observed. Non-structural Ti(IV)/Fe(II) amorphous phase on the x = 0.5 and 0.75 nanoparticle surface can also be seen, in agreement with previous study,[10] where Ti was expected to be incorporated in magnetite only up to x = 0.38.

Reduction of 4-NP and NB by titanomagnetite. The reduction of 4-NP by titanomagnetite was carried out in 250 mL Nalgene™ polypropylene bottles under anaerobic conditions (glovebox). Sample volume was 200 mL. All experiments were conducted under constant magnetic stirring (1400 rpm), a stirring speed that effectively ensured a homogeneous suspension according to preliminary tests. Variations in pH, Eh, [4-NP], [4-AP] and $[Fe(II)]_{aq}$ during the reaction were monitored. At each sampling time, an aliquot was taken and filtered (0.2 μm, Whatman) for high performance liquid chromatography analysis with UV-vis detection (HPLC-UV; for [4-NP] and [4-AP]) and dissolved Fe(II) analysis (by the phenanthroline method). Mobile phase for HPLC was a mixture of 50% ultrapure water, 50% acetonitrile (HPLC grade, J.T. Baker, USA), and 1% formic acid. [4-NP] and [4-AP] were measured at a flow rate of 1.0 mL min^{-1} at wavelengths of

317 nm and 273 nm, respectively. In addition, changes of [4-NP] was measured for some series of experiments by UV-vis spectrophotometry (CARY 50 probe, Varian) at 400 nm. Filtered samples were diluted by 10 in 50 mM 3-(N-morpholino) propanesulfonic acid (MOPS) (pH = 8) for UV-vis analysis. Both methods (HPLC and UV-vis spectrophotometry) were in excellent agreement. Experimental errors on [Fe(II)], [4-NP] and [4-AP] determination were 5% in the worst case, as also confirmed by duplicating the experiments. As a conservative approach, standard deviations on the rate constants were determined assuming 5% uncertainty on [4-NP] determination.

pH and Eh were recorded in both titanomagnetite and Fe(II)-amended magnetite suspensions using a portable multi-parameter electrode (pH, Eh and T; Hach, sensION+5045). The pH electrode was calibrated with 3 standard buffers (pH 4, 7 and 10). The Pt-electrode combined with a Ag/AgCl reference electrode, used for redox potential measurements, was calibrated using a commercial redox-buffer (220 mV vs Ag/AgCl). Raw data were converted into Eh vs. standard hydrogen electrode (SHE) by correcting for the potential of the reference electrode. Note that measured Eh values are only used as qualitative indication in this study.

Experiments were conducted in buffered pH systems using 50 mM MOPS, which is a commonly used pH-buffer in Fe-based redox reactions studies.[1-4,7,8] All experiments were conducted at pH = 8, except when pH effects were investigated. The titanomagnetites suspensions were pre-equilibrated during 60 min, together with the multi-parameter electrode, to ensure a stable Eh reading (see e.g. Fig. S3). After noting pH and Eh values at the end of these 60 min, 0.1 mM 4-NP (or 10 μM 4-NP, for some experiments) was spiked into the suspension. Final pH and Eh values were taken after immersing the multi-parameter electrode in the batch during the last 60 min of the experiment (i.e. from 180 to 240 min). The effect of Ti content on 4-NP reduction (x = 0, 0.25, 0.38, 0.5 and 0.75) was investigated at pH = 8 for 200 mg L^{-1}

(titano)magnetite (0.76, 1.06, 1.20, 1.31 and 1.53 mM Fe(II) equivalent, respectively). For all experimental conditions, the amount of Fe(II) equivalent was larger than electron equivalent amount required for the complete reduction of 4-NP (i.e. 0.6 meq of electron for 0.1 mM 4-NP).

To facilitate the comparison between magnetite and titanomagnetite, Fe(II) was added to magnetite suspension in order to have an equal amount of total Fe(II), so that the initial concentration of Fe(II) in each of the $Fe_{3-x}Ti_xO_4$ experiments was equal to the initial concentration of Fe(II) (added Fe(II) + solid Fe(II)) in the magnetite experiments. Indeed, experiments using magnetite amended with Fe(II) (using a 100 mM $FeCl_2$ solution in 0.1 M HCl) were conducted at pH = 8 (MOPS) for the same amounts of Fe(II) equivalent than for titanomagnetites (i.e. by adding dissolved Fe(II) to reach 1.06, 1.20, 1.31 and 1.53 mM Fe(II) equivalent), and are denoted M+Fe(II). The effect of pH ($6 \leq pH \leq 8.5$) on 4-NP reduction was investigated for 200 mg L^{-1} TiM0.5 and M+Fe(II) (1.31 mM Fe(II) equivalent). Although MOPS has a weak buffer capacity for $pH < 6.2$ and $pH > 8.2$ ($pK_a = 7.2$), it was used in all experiments for the sake of consistency of the dataset. No significant pH variation was observed during the experiments, even outside the pH-buffering range of MOPS. Other experiments were conducted at different suspension loading (100, 250, 600 mg L^{-1}) applying the same protocol.

One experiment was carried out with TiM0.5 in the absence of pH buffer. The multi-parameter electrode was kept in the sample during the complete experiment. 200 mg L^{-1} TiM0.5 (1.31 mM Fe(II) equivalent) were introduced in ultrapure water, whose pH was adjusted to pH = 8.4 (around the natural pH of the mother TiM0.5 suspension) with 0.1 M NaOH prior to the addition of TiM0.5. $[Fe(II)]_{aq}$, pH and Eh were recorded until pH and Eh values reached a plateau (~60 min). Then, 0.1 mM 4-NP (10 mM 4-NP stock solution adjusted to pH = 8.4) was spiked into the suspension, which is taken as the reference for the time scale (t = 0). [4-NP] and [4-AP] were recorded during the four following hours (240 min), in addition to $[Fe(II)]_{aq}$, pH and Eh.

Further experiments were dedicated to nitrobenzene (NB) reduction by titanomagnetite or Fe(II)-amended magnetite. The effect of x was investigated using the same conditions as in 4-NP experiments (i.e. 0.1 mM NB, 200 mg L^{-1} solid, pH = 8, in 50 mM MOPS), and NB concentration was determined by HPLC-UV at 254 nm.

Because of the weak sorption of 4-NP or NB and its rapid reduction, an accurate determination of sorbed amount by magnetite or titanomagnetite surfaces cannot be performed. Attempts to highlight the sorbed mechanisms at a microscopic level by using Attenuated Total Reflectance-Fourier Transform InfraRed (ATR-FTIR) spectroscopy failed due to the very low sorbed amount.

Results and Discussion

Reduction of 4-NP by titanium-substituted magnetites. The reductive transformation of 4-NP to 4-AP in aqueous suspension was monitored versus time by both UV-Visible spectrophotometer and HPLC/UV. The time-dependent UV-vis spectra exhibited a peak at 400 nm (4-NP), which continuously decreased with the formation of a single new peak at 298 nm, assigned to 4-AP (not shown).[21] The absence of peaks at 388 and 302 nm (which can correspond to 4-benzoquinone monoxime and 4-nitrosophenol[22]) together with the two isosbestic points observed at 280 and 312 nm suggested that no other byproducts were generated.[23] HPLC analysis confirmed the stoichiometric conversion of 4-NP to 4-AP, as [4-NP] + [4-AP] = 0.1 mM (within 5% uncertainty; see e.g. Fig. S3), indicating that mass balance was achieved and removal of 4-NP or 4-AP by sorption on magnetite surfaces must be negligible.

Figure 1a shows that the 4-NP reduction was enhanced with the increase of Ti content in $Fe_{3-x}Ti_xO_4$ ($0 \leq x \leq 0.75$) (or the increase of the Fe(II)/Fe(III) ratio, Table 1). The kinetic curves

exhibited a fast stage within the first 10-15 min, and then a slower stage to reach a pseudo-plateau (Fig. 1a). According to experiments conducted at longer equilibration times (e.g. 48h, not shown), 4-NP aqueous concentration still slightly and slowly decreased beyond 240 min, which is in line with observations made for other compounds[11]. In contrast to previous reports on 4-NP reduction,[24,25] the multi-stage reduction kinetics over the whole time course could not be described by equations that include classical exponential functions (e.g. first order models). Instead, we calculated an initial rate constant (k_{obs} in min^{-1}) over the first stage of reaction (i.e. 10 min) by plotting a linear regression of $-\ln([4\text{-NP}]/[4\text{-NP}]_0)$ versus time, as previously used for other $Fe_{3-x}Ti_xO_4$-mediated reactions.[11] This behavior has been attributed to the complexity of involved reactions including simultaneous dissolution of Fe(II), movement of Fe(II) reducing equivalents from the interior to the surface and reduction/oxidation processes at the interface.[10,11] Additionally, the occurrence of Fe(II)/Ti(IV) amorphous phases observed at higher x values (i.e. > 0.38) may affect the reduction behavior, as previously reported.[11] However, the contribution of the latter has been only observed for the reduction of 10 μM of Tc(VII) to Tc(IV) and became negligible for larger oxidant amounts (e.g. 30 μM of Tc(VII)).[11] In the present work, similar kinetic behavior was obtained when a lower amount of oxidant (i.e. 10μM of 4-NP instead of 100 μM) was used (Fig. S4a), thereby underscoring the low contribution of such amorphous phases.

Figure 1b shows that higher $[Fe(II)]_{aq}$ was measured for larger x and that a gradual decrease in $[Fe(II)]_{aq}$ was observed throughout the 4-NP reduction. $[Fe(II)]_{aq}$ was below the detection limit in magnetite suspension (x=0), where no 4-NP reduction was noted. Consistently, initial measured Eh values decreased with x ($-154 < Eh < -383$ mV, for $0 \leq x \leq 0.75$; Table S1) and, at the end of all experiments, less negative (or almost equal for x=0) Eh values were measured ($-145 < Eh < -240$ mV; Table S1), though Eh values have to be interpreted only qualitatively. Homogeneous tests using Fe(II) solutions (1mM or less of [Fe(II)] as $FeCl_2$) at pH

= 8 did not show a significant removal of 4-NP within 240 min, suggesting that 4-NP reduction in $Fe_{3-x}Ti_xO_4$ suspensions is a surface-mediated electron transfer process.

Because Fe(II) release in solution was observed, titanomagnetite-bound [Fe(II)] (i.e. structural/sorbed Fe(II)) before 4-NP addition was calculated as follows: $[Fe(II)]_{bound} = [Fe(II)]_{tot} - [Fe(II)]_{aq}$, and was found very close to that determined by acid digestion on the filtered solid. This value was used to calculate $(Fe(II)/Fe(III))_{bound}$, that is, the effective Fe(II):Fe(III) ratio in the solid phase (see Table S1). Although the Fe(II)/Fe(III) ratio is known to be the thermodynamic driving force for electron transfer from magnetite to substrate, a logarithmic dependence of rate constants with increasing $(Fe(II)/Fe(III))_{bound}$ was observed (Fig. 2a). Use of a lower amount of oxidant (i.e. 10 μM of 4-NP) gave the same type of relationship, i.e. a nonlinear dependence of k_{obs} with Fe(II)/Fe(III) (Fig. S4a). However, k_{obs} or amounts of 4-NP removed at the end of the experiment (240 min) linearly correlated to the amount of initial Fe(II) in each suspension (Fig. 2b, S4b and S5, respectively). Linear correlations were also found out by plotting k_{obs} versus x or measured initial Eh (Fig. S6). Systematic correlation of reduction rates with x clearly showed that 4-NP reduction is mainly controlled by a surface-mediated electron transfer pathway. Additional tests made for different TiM0.5 suspension loading (100-250 mg L^{-1}) showed that k_{obs} or total amounts of 4-NP linearly increased with the suspension loading (Fig. 3a, 3c), further suggesting that 4-NP reduction in titanomagnetite suspensions is a surface-mediated reaction. The dissolved Fe(II) concentration, that was initially higher for the highest suspension loading, gradually decreased throughout the reaction (Fig. 3b).

Note that pH = 8 is 1-2 pH units above the PZC value (pH 6-7[10]), and most of magnetite particles are negatively charged, inducing a significant stability of colloidal dispersions. Increase of electrolyte concentrations promotes charge screening, decrease of repulsive forces and, ultimately, particles aggregation.[26] Investigation of 4-NP reduction kinetics in the presence of

high monovalent electrolyte concentrations (1M NaCl) did not significantly influence neither the reduction kinetics (i.e. 4-NP decay vs. time) nor the relationship of k_{obs} with $(Fe(II)/Fe(III))_{bound}$ (Fig. S7), suggesting that the impact of aggregation phenomena on 4-NP reduction kinetics in titanomagnetite suspensions is of minor importance.

As a further test of whether the molecular structure of the substrate can affect the reduction behavior of titanomagnetite, we determined removal kinetics in the same manner but by using nitrobenzene (NB) as a target compound. While the reduction of NB was found faster (Fig. 2a and 2b), a nonlinear dependence of k_{obs} with $(Fe(II)/Fe(III))_{bound}$ was observed for NB as for 4-NP (Fig. 2a), suggesting that specific molecular interactions do not play a significant role in the determination of relationship of k_{obs} with Fe(II)/Fe(III). The latter has been recently explained by employing the Marcus' theory of electron transfer reactions.[12] The k_{obs} values increase with increasing $(Fe(II)/Fe(III))_{bound}$ and exponentially approach a plateau as the magnitude of the reaction free energy becomes close to the value of the reorganization energy of the adsorbed compound assumed constant along the reaction.[27]

Effect of pH on 4-NP reduction in titanomagnetite suspensions. As pH is a key reaction parameter that strongly affects the aqueous iron chemistry and consequently the reductive capability of Fe^{II}-bearing minerals, we determined removal kinetics in a pH range from 6 to 8.5 in titanomagnetite suspensions (x=0.5) (Fig. S8). k_{obs} values increased when pH rose up to pH 8 and then remained almost constant beyond pH 8 (i.e. 8.5) (Fig. 4a). A slight decrease in 4-NP removal extent can be observed at pH 8.5 (Fig. S8a), as the protonated form of 4-NP ($pK_a \approx 7.1$) was shown to favor the reduction of its nitro group.[28] Generally, magnetite reactivity can be enhanced at high pH values, which has been attributed to the preservation of structural Fe(II) against dissolution, and/or the improvement in Fe(II) adsorption on the surface.[7,23] Indeed,

$[Fe(II)]_{aq}$ was initially higher at lower pH values, gradually decreased throughout the 4-NP reduction at pH 8, and became below the detection limit within less than 60 min at pH = 8.5 (Fig. S8b). For pH ≤ 7.5, no decrease in $[Fe(II)]_{aq}$ was observed with time, which can be explained by the H^+ promoted dissolution of titanomagnetite, and the small or no-reductive conversion of 4-NP to 4-AP. It should be noted that the 4-NP adsorption to titanomagnetite surfaces was found negligible (< 5%) whatever the pH tested. To assess the effect of MOPS pH-buffer on Fe(II) dissolution and then its reactivity (as previously highlighted),[29,30] unbuffered experiments were conducted at initial pH of 8.4 (pH only slightly varied (8.3 ± 0.1 (1σ), details is given in SI). Comparison of buffered versus unbuffered pH systems for 8 ≤ pH ≤ 8.5 shows that MOPS increased significantly the Fe(II) apparent solubility, but did not affect the 4-NP removal (Fig. S3). Indeed, k_{obs} determined in the unbuffered system follows a consistent trend with pH (see open symbol in Fig. 4a).

A linear relationship was obtained between k_{obs} and $[Fe(II)]_{bound}$ ($R^2 = 0.92$) in the series of experiments dedicated to the effect of pH (for x = 0.5) and the effect of x (for pH = 8) (Fig. 4b). Collectively, these results clearly demonstrated that the Fe(II)/Fe(III) ratio effectively controls the surface-mediated reduction of 4-NP and its conversion to 4-AP, and that the mechanism is mainly driven by structural or surface bound Fe(II) in the titanomagnetite. This conclusion has been previously drawn for magnetite and Ti-substituted magnetite, but also for non-stoichiometric magnetite amended with Fe(II) aiming to increase the intrinsic Fe(II)/Fe(III) ratio (see e.g. [2-4,7,8,11,13]). However, the reduction kinetics and mechanisms in Ti-magnetite *versus* Fe(II)-amended magnetite at equal amounts of Fe(II) equivalent have never been investigated.

Effects of $Fe(II)_{aq}$ addition on the reactivity of magnetite (x = 0). 4-NP reduction by Fe(II)-amended magnetite is compared with the data of titanomagnetites in the same range of total

Fe(II) equivalent (from 0.76 to 1.53 mM) in Figure 1a. As expected, addition of dissolved Fe(II) to non-stoichiometric magnetite (Fe(II)/Fe(III) = 0.41, Table 1) significantly enhanced the 4-NP reduction rate. However, 4-NP reduction proceeded faster in the case of Fe(II)-amended magnetite than with titanomagnetite, and reached quickly a pseudo-plateau within the first 5 min. Like with titanomagnetites, we focused only on the initial stage kinetic, though 4-NP concentration still decreased slightly and slowly beyond 240 min. Initial k_{obs} and 4-NP removed amounts after 240 min were plotted versus initial Fe(II) equivalent in Figures 2b and S5, respectively. Initial k_{obs} is shown to increase exponentially with $(Fe(II)/Fe(III))_{bound}$ (Fig. 2a), as previously observed for the reduction of nitroaromatic compounds by magnetite,[4] which strongly contrasts with the observation made for titanomagnetites. However, k_{obs} increased linearly with the amount of initial Fe(II) equivalent for Fe(II)-amended magnetites, but with larger k_{obs} values (Fig. 2b).

It is interesting to note that similar removed amounts of 4-NP at the end of experiment (i.e. 240 min) were achieved whatever the investigated system: titanomagnetite, Fe(II)-amended magnetite or Fe(II) amended-TiM0.25, provided only that the same amount of total Fe(II) equivalent was used. When the removed amounts were plotted against total Fe(II) equivalent, similar slope and intercept of the linear regression equations were obtained (see Fig. S5). This falls in line with previous findings where the extent of U(VI) reduction by magnetite or titanomagnetite was found only controlled by the bulk Fe(II)/Fe(III) ratio, and the presence of Ti did not significantly influence the effective reductive capacity[13]. Only the early stage kinetic behavior differs between titanomagnetite and Fe(II)-amended magnetite at the same equivalent amount of Fe(II). This kinetic discrepancy became salient when higher solid loadings, e.g. 600 mg L^{-1} of TiM0.25 or Fe(II)-amended magnetite (3.18 mM Fe(II) equivalent), were used (Fig. S9). Since this discrepancy was observed for all x values, the possible contribution of

Fe(II)/Ti(IV) amorphous phases (the occurrence of which is only expected at high x values) can be neglected. The same kinetic discrepancy was observed for the reduction of 0.1 mM NB (where rates are close to published data on magnetite[4]), and thus independent on the investigated substrate (Fig. 2). Like for 4-NP experiments, only the kinetic behavior differs between titanomagnetite and Fe(II)-amended magnetite, and NB removed amounts after 240 min were found very close (data not shown).

Modification of aggregation state of particles may occur upon Fe(II) adsorption at pH=8, which might, in turn, affect 4-NP and NB reduction kinetics. However, cation sorption to the negatively charged surface (PZC 6-7) would lead to more aggregation in aqueous suspensions at pH=8.[26] Such homoaggregation is supposed to rather decrease surfaces reactivity,[31] and thus cannot help to explain the high reduction rates of 4-NP and NB in Fe(II)-magnetite suspensions with respect to the titanomagnetite. Furthermore, repeated experiments in 1 M NaCl solution did not affect significantly 4-NP reduction rates (Fig. S7). The higher reactivity of Fe(II)-amended magnetite system over titanomagnetite was then confirmed at different pH values (6.3, 7, 8, 8.5) for 4-NP. Similarly to titanomagnetites, k_{obs} increased with increasing pH but with higher values over the pH-range investigated (Fig. 4a). Furthermore, different linear relationships were obtained by plotting k_{obs} with the amount of initial Fe(II) equivalent (Fig. 2b), thereby confirming the kinetic discrepancy between magnetite and titanomagnetite. Previous works have suggested that the presence of Ti may lead to changes in surface speciation of radionuclides (Tc(VII), U(VI) and Np(V)[11,13,14]), but they did not highlight the impact of Ti substitution on the reduction kinetics. This unforeseen disparity in reduction kinetics between titanomagnetite and Fe(II)-amended magnetite, though the total Fe(II) amount is identical, will be discussed in the following paragraph.

Reactivity difference between the Fe(II) + unsubstituted magnetite and Ti-magnetite. It is postulated that the added Fe(II) binds to non-stoichiometric magnetite, and then oxidation of the sorbed Fe(II) and subsequent reduction of the octahedral Fe(III) in the underlying magnetite to octahedral Fe(II) atoms take place. This process occurs until saturation of magnetite (i.e. formation of stoichiometric magnetite, Fe(II)/Fe(III) ~ 0.5), thus enhancing the reductive ability of the resulting product.[3] Formation of new Fe-phase was not observed upon addition of dissolved Fe(II) to magnetite.[3] Our measurements of both dissolved and solid Fe(II) confirmed that nearly-stoichiometric magnetite was formed before addition of 4-NP in all Fe(II)-amended magnetite experiments. Because excess dissolved Fe(II) was not removed from the suspensions, it could supply magnetite surface when oxidized by 4-NP to regenerate active sites, as previously reported for magnetite[2] and Fe(III)-oxides.[32-34] This is consistent with the sharp fall in $[Fe(II)]_{aq}$ after 4-NP addition to magnetite suspensions (see e.g. Fig. 1b) and explains why larger rate constants were obtained for larger added [Fe(II)]. For titanomagnetites, though most of Fe(II) is *a priori* supposed to be in the bulk structure, there is still an abundant amount of Fe(II) at the surface according to previous studies.[10,11,16] In addition, initial amounts of dissolved Fe(II) in one hour pre-equilibrated titanomagnetite suspensions were found to be relatively large, and only slightly lower than in the corresponding Fe(II)-amended magnetite experiments (see e.g. Fig. 1b). Thus there should be enough dissolved Fe(II) to supply the surface of titanomagnetite when oxidized by 4-NP. Furthermore, $[Fe(II)]_{aq}$ decrease appears more gradual for titanomagnetites than for Fe(II)-amended magnetite (Fig. 1b), thereby confirming the slow kinetics of the former. Fe(II) addition to TiM0.25 suspension, in order to have the same equivalent amount of Fe(II) as in TiM0.5, resulted in faster reduction rates of 4-NP (k_{obs} = 0.08±0.01 min^{-1}) than with TiM0.5 (k_{obs} = 0.05±0.01 min^{-1}) but slower than with the corresponding magnetite + Fe(II) (k_{obs} = 0.14±0.02 min^{-1}) (Fig. S10). Similar observations can be made for TiM0.75 (Fig. S11, see also

Fig. S5-7). Taken together, these findings further suggested that although oxide surfaces are saturated with a supply of Fe(II), the Ti-substitution may affect the reduction kinetics behavior of 4-NP.

The surface-mediated reduction of 4-NP implies an electron transfer mechanism through the particles, thus rendering it a bulk dependent effect. Indeed, an electron transport process must be enlisted to enable redox reaction to proceed at magnetite surfaces, transferring charge through the core via an electron transfer mechanism to the surface of the magnetite.[3,10,15] Within the magnetite, the existence of interactions between octahedral cations (i.e. Fe^{2+} and Fe^{3+}) is responsible of electron delocalization or hopping, creating a net charge of +2.5.[35] Any modification with a tendency to increase the repulsion between octahedral sites must result in a relative shortening of the shared octahedral edge, and so declining in electron delocalization or hopping. The possible presence of Ti^{4+} ions in octahedral sites may result in relatively greater repulsion between the octahedral cations, which lead to a localization of electrons (otherwise mobile for Fe^{3+}-Fe^{2+} pairs)[36-39]. Consequently, electron transfer process both within the solid phase and across the solid/water interface, that ensures surface regeneration of active sites and ongoing 4-NP reduction, seems to be kinetically more favored (*i.e.* a lower barrier in terms of activation energy) in the Fe(II)-amended unsubstituted magnetite.

Conclusions

In this work, we have notably demonstrated that, although both surfaces are highly enriched in Fe(II), faster reduction rate constants of nitroaromatic compounds were obtained for Fe(II)-amended unsubstituted magnetite as compared to the Ti-substituted magnetite. The partial occupancy of octahedral sites by Ti may change interactions between octahedral cations (*e.g.* Fe^{2+} and Fe^{3+} in case of unsubstituted magnetite), and then electron delocalization properties or

electron hopping. These bulk-controlled mechanisms drive the electron transfer process both within the solid phase and across the solid/water interface, thereby altering the regeneration of active sites and ongoing 4-NP reduction on the magnetite surface.

From a kinetic point of view, Fe(II)-amended magnetite may have some advantages for the conversions of 4-NP and NB to, respectively, 4-AP and aniline over titanomagnetite. Indeed, a highly reactive system (i.e. faster rate constants) could allow better performance in a short period time, which is crucial to successfully ensure scaling-up an environmental remediation technology.

Collectively, these results may have strong implications for (i) mass reduction of 4-NP to 4-AP without involving more expensive transition metals and (ii) remediation of contaminated water and wastewater where Fe(II)-recharge of magnetite could be environmental-friendly and economically-feasible, with respect to the titano-doping of magnetite.

Acknowledgements

The authors gratefully acknowledge the financial support of this work by ADEME “Agence de l'Environnement et de la Maîtrise de l'Energie” N° of funding decision 1472C0030.

Supporting Information Available

Details of the synthesis and characterization of titanomagnetites; 4-NP reduction in unbuffered pH system, and other reduction data at different experimental conditions. This information is available free of charge via the Internet at http://pubs.acs.org/.

References

(1) Heijman, C. G.; Holliger, C.; Glaus, M. A.; Schwarzenbach, R. P.; Zeyer J. Abiotic Reduction of 4-Chloronitrobenzene to 4-Chloroaniline in a Dissimilatory Iron-Reducing Enrichment Culture. *Appl. Environ. Microbiol.* **1993**, *59*, 4350–4353.

(2) Klausen, J.; Tröber, S. P.; Haderlein, S. B.; Schwarzenbach, R. P. Reduction of Substituted Nitrobenzenes by Fe(ll) in Aqueous Mineral Suspensions. *Environ. Sci. Technol.* **1995**, *29*, 2396–2404.

(3) Gorski, C. A.; Scherer M. M. Influence of Magnetite Stoichiometry on Fe^{II} Uptake and Nitrobenzene Reduction. *Environ. Sci. Technol.* **2009**, *43*, 3675–3680.

(4) Gorski, C. A.; Nurmi, J. T.; Tratnyek P. G.; Hofstetter T. B.; Scherer M. M. Redox Behavior of Magnetite: Implications for Contaminant Reduction. *Environ. Sci. Technol.* **2010**, *44*, 55–60.

(5) McCormick, M. L.; Bouwer, E. J.; Adriaens, P. Carbon Tetrachloride Transformation in a Model Iron-Reducing Culture: Relative Kinetics of Biotic and Abiotic Reactions. *Environ. Sci. Technol.* **2002**, *36*, 403–410.

(6) McCormick, M. L.; Adriaens, P. Carbon Tetrachloride Transformation on the Surface of Nanoscale Biogenic Magnetite Particles. *Environ. Sci. Technol.* **2004**, *38*, 1045–1053.

(7) Gregory, K. B.; Larese-Casanova, P.; Parkin, G. F.; Scherer, M. M. Abiotic Transformation of Hexahydro-1,3,5-trinitro-1,3,5-triazine by Fe^{II} Bound to Magnetite. *Environ. Sci. Technol.* **2004**, *38*, 1408–1414.

(8) Latta, D. E.; Gorski, C. A.; Boyanov, M. I.; O'Loughlin, E. J.; Kemner, K. M.; Scherer, M. M. Influence of Magnetite Stoichiometry on U^{VI} Reduction. *Environ. Sci. Technol.* **2012**, *46*, 778−786.

(9) Cornell, R. M.; Schwertmann, U. *The Iron Oxides: Structure, Properties, Reactions, Occurrences, And Uses*; Wiley-VCH: Weinheim, 2003.

(10) Pearce, C. I.; Qafoku, O.; Liu, J.; Arenholz, E.; Heald, S. M.; Kukkadapu, R. K.; Gorski, C. A.; Henderson, C. M. B.; Rosso, K. M. Synthesis and Properties of Titanomagnetite ($Fe_{3-x}Ti_xO_4$) Nanoparticles: A Tunable Solid-State Fe(II/III) Redox System. *J. Coll. Int. Sci.* **2012**, *387*, 24–38.

(11) Liu, J.; Pearce, C. I.; Qafoku, O.; Arenholz, E.; Heald, S. M.; Rosso, K. M. Tc(VII) Reduction Kinetics by Titanomagnetite ($Fe_{3-x}Ti_xO_4$) Nanoparticles. *Geochim. Cosmochim. Acta* **2012**, *92*, 67–81.

(12) Liu, J.; Pearce, C. I.; Liu, C.; Wang, Z.; Shi, L.; Arenholz, E.; Rosso, K. M. $Fe_{3-x}Ti_xO_4$ Nanoparticles as Tunable Probes of Microbial Metal Oxidation. *J. Am. Chem. Soc.* **2013**, *135*, 8896–8907.

(13) Latta, D. E.; Pearce, C. I.; Rosso, K. M.; Kemner, K. M.; Boyanov, M. I. Reaction of U^{VI} with Titanium-Substituted Magnetite: Influence of Ti on U^{IV} Speciation. *Environ. Sci. Technol.* **2013**, *47*, 4121−4130.

(14) Wylie, M. E.; Olive, D. T.; Powell, B. A. Effects of Titanium Doping in Titanomagnetite on Neptunium Sorption and Speciation. *Environ. Sci. Technol.* **2016**, *50*, 1853–1858.

(15) White, A. F.; Peterson, M. L.; Hochella M. F. Jr. Electrochemistry and Dissolution Kinetics of Magnetite and Ilmenite. *Geochim. Cosmochim. Acta* **1994**, *58*, 1859–1875.

(16) Pearce, C. I.; Liu, J.; Baer, D. R.; Qafoku, O.; Heald, S. M.; Arenholz, E.; Grosz, A. E.; McKinley, J. P.; Resch, C. T.; Bowden, M. E. et al. Characterization of Natural Titanomagnetites ($Fe_{3-x}Ti_xO_4$) for Studying Heterogeneous Electron Transfer to Tc(VII) in the Hanford Subsurface. *Geochim. Cosmochim. Acta* **2014**, *128*, 114–127.

(17) Yang, S.; He, H.; Wu, D.; Chen, D.; Liang, X.; Qin, Z.; Fan, M.; Zhu, J.; Yuan, P. Decolorization of Methylene Blue by Heterogeneous Fenton Reaction Using $Fe_{3-x}Ti_xO_4$ ($0 \leq x \leq 0.78$) at Neutral pH Values. *Applied Catalysis B: Environmental* **2009**, *89*, 527–535.

(18) Zhong, Y.; Liang, X.; Zhong, Y.; Zhu, J.; Zhu, S.; Yuan, P.; He, H.; Zhang, J. Heterogeneous UV/Fenton Degradation of TBBPA Catalyzed by Titanomagnetite: Catalyst Characterization, Performance and Degradation Products. *Water Research* **2012**, *46*, 4633–4644.

(19) Fortune, W. B.; Mellon, M. G. Determination of Iron with o-phenanthroline-A Spectrophotometric Study. *Ind. Eng. Chem. Anal. Ed.* **1938**, *10*, 0060−0064.

(20) Rodriguez-Carvajal, J. Recent Advances in Magnetic-Structure Determination by Neutron Powder Diffraction. *Physica B* **1993**, *192*, 55–69.

(21) Lin, F. H.; Doong, R. A. Bifunctional Au-Fe_3O_4 Heterostructures for Magnetically Recyclable Catalysis of Nitrophenol Reduction. *J. Phys. Chem. C* **2011**, *115*, 6591−6598

(22) Velghe, N.; Claeys, A. Rapid Spectrophotometric Determination of Nitrate with Phenol. *Analyst* **1983**, *108*, 1018−1022.

(23) Bae, S.; Hanna, K. Reactivity of Nanoscale Zero-Valent Iron in Unbuffered Systems: Effect of pH and Fe(II) Dissolution. *Environ. Sci. Technol.* **2015**, *49*, 10536–10543.

(24) Zheng, J.; Dong, Y.; Wang, W.; Ma, Y.; Hu, J.; Chen X.; Chen, X. In Situ Loading of Gold Nanoparticles on Fe_3O_4@SiO_2 Magnetic Nanocomposites and Their High Catalytic Activity. *Nanoscale* **2013**, *5*, 4894–4901.

(25) Safari, J.; Gandomi-Ravandi, S.; Haghighi, Z. Supported Polymer Magnets with High Catalytic Performance in the Green Reduction of Nitroaromatic Compounds. *RSC Adv.* **2016**, *6*, 31514–31525.

(26) Huynh, K. A.; Chen, K. L. Aggregation Kinetics of Citrate and Polyvinylpyrrolidone Coated Silver Nanoparticles in Monovalent and Divalent Electrolyte Solutions. *Environ. Sci. Technol.* **2011**, *45*, 5564–5571.

(27) Marcus, R. A.; Sutin, N. Electron Transfers in Chemistry and Biology. *Biochim. Biophys. Acta* **1985**, *811*, 265–322.

(28) Schwarzenbach, R. P.; Stierli, R.; Lanz, K.; Zeyer, J. Quinone and Iron Porphyrin Mediated Reduction of Nitroaromatic Compounds in Homogeneous Aqueous Solution. *Environ. Sci. Technol.* **1990**, *24*, 1566–1574.

(29) Stemig, A. M.; Do, T. A.; Yuwono, V. M.; Arnold, W. A.; Penn, R. L. Goethite Nanoparticle Aggregation: Effects of Buffers, Metal Ions, and 4-Chloronitrobenzene Reduction. *Environ. Sci.: Nano* **2014**, *1*, 478–487.

(30) Buchholz, A.; Laskov, C.; Haderlein S. B. Effects of Zwitterionic Buffers on Sorption of Ferrous Iron at Goethite and Its Oxidation by CCl_4. *Environ. Sci. Technol.* **2011**, *45*, 3355–3360.

(31) Hochella, M. F. Jr.; Lower, S. K.; Maurice, P. A.; Penn, R. L.; Sahai, N.; Sparks, D. L.; Twining, B. S. Nanominerals, Mineral Nanoparticles, and Earth Systems. *Science* **2008**, *319*, 1631–1635.

(32) Amonette, J. E.; Workman, D. J.; Kennedy, D. W.; Fruchter, J. S.; Gorby, Y. A. Dechlorination of Carbon Tetrachloride by Fe(II) Associated with Goethite. *Environ. Sci. Technol.* **2000**, *34*, 4606–4613.

(33) Pecher, K.; Haderlein, S. B.; Schwarzenbach, R. P. Reduction of Polyhalogenated Methanes by Surface-Bound Fe(II) in Aqueous Suspensions of Iron Oxides. *Environ. Sci. Technol.* **2002**, *36*, 1734–1741.

(34) Williams, A. G. B.; Scherer, M. M. Spectroscopic Evidence for Fe(II)−Fe(III) Electron Transfer at the Iron Oxide−Water Interface. *Environ. Sci. Technol.* **2004**, *38*, 4782–4790.

(35) Tanaka, H.; Kono, M. Mossbauer Spectra of Titanomagnetite: A Reappraisal. *J. Geomag. Geoelectr.* **1987**, *39*, 463–475.

(36) Walz, F.; Torres, L.; Bendimya, K.; de Francisco, C.; Kronmüller, H. Analysis of Magnetic After-Effect Spectra in Titanium-Doped Magnetite. *Phys. Stat. Sol. (a)* **1997**, *164*, 805–820.

(37) Brabers, V. A. M. The Electrical Conduction of Titanomagnetites. *Physica B* **1995**, *205*, 143–152.

(38) Wechsler, B. A.; Lindsley, D. H.; Prewitt, C. T. Crystal Structure and Cation Distribution in Titanomagnetites ($Fe_{3-x}Ti_xO_4$). *American Mineralogist* **1984**, *69*, 754–770.

(39) Guigue-Millot, N.; Champion, Y.; Hyltch, M. J.; Bernard, F.; Begin-Colin, S.; Perriat, P. Chemical Heterogeneities in Nanometric Titanomagnetites Prepared by Soft Chemistry and Studied Ex Situ: Evidence for Fe-Segregation and Oxidation Kinetics. *J. Phys. Chem. B* **2001**, *105*, 7125–7132.

Table 1. Expected and experimental Fe(II)/Fe(III) ratio, B.E.T. surface area of titanomagnetites, crystallite size and cell parameter determined by XRD analysis.

	Fe(II)/Fe(III)		B.E.T.	Cristallite	Cell parameter
x	Expected	Chemical analysis	($m^2\ g^{-1}$)	size (nm)	(Å)
0	0.50	0.41	95	9	8.384(2)
0.25	0.83	0.80	118	10	8.384(2)
0.38	1.11	1.08	144	13	8.396(2)
0.50	1.50	1.48	139	13	8.397(2)
0.75	3.50	3.26	132	28	8.413(2)

Figure captions

Figure 1. Effect of titanomagnetite stoichiometry ($Fe_{3-x}Ti_xO_4$; $0 \leq x \leq 0.75$; 200 mg L^{-1}) and dissolved Fe(II) added to 200 mg L^{-1} magnetite (for comparable Fe(II) equivalent) on the reduction of 0.1 mM 4-NP at pH = 8 (50 mM MOPS): (a) 4-NP concentration and (b) dissolved Fe(II) concentration versus time. Same symbols and legends are used in (a) and (b).

Figure 2. Initial rate constant (k_{obs}) versus (a) $(Fe(II)/Fe(III))_{bound}$ and (b) initial Fe(II) equivalent for the reduction of 4-NP (0.1 mM) or NB (0.1 mM) by 200 mg L^{-1} titanomagnetite ($0 \leq x \leq 0.75$) and Fe(II)-amended magnetite at pH = 8 (50 mM MOPS).

Figure 3. Effect of the suspension loading for x = 0.5 on the reduction of 0.1 mM 4-NP by titanomagnetite (x = 0.5) at pH = 8 (50 mM MOPS). (a) 4-NP concentration and (b) dissolved Fe(II) concentration versus time, (c) initial rate constant (k_{obs}) versus suspension loading.

Figure 4. (a) Initial rate constant (k_{obs}) versus pH determined for the reduction of 0.1 mM 4-NP by 200 mg L^{-1} TiM0.5 and 200 mg L^{-1} magnetite amended with 0.56 mM Fe(II) (1.31 mM Fe(II) equivalent in both systems). The empty square corresponds to unbuffered pH system (see Fig. S3). (b) Initial rate constant (k_{obs}) versus initial $[Fe(II)]_{bound}$ for the experiments dedicated to 4-NP reduction by 200 mg L^{-1} titanomagnetite (effects of pH for x = 0.5, and effects of x for pH = 8).

Figure 1

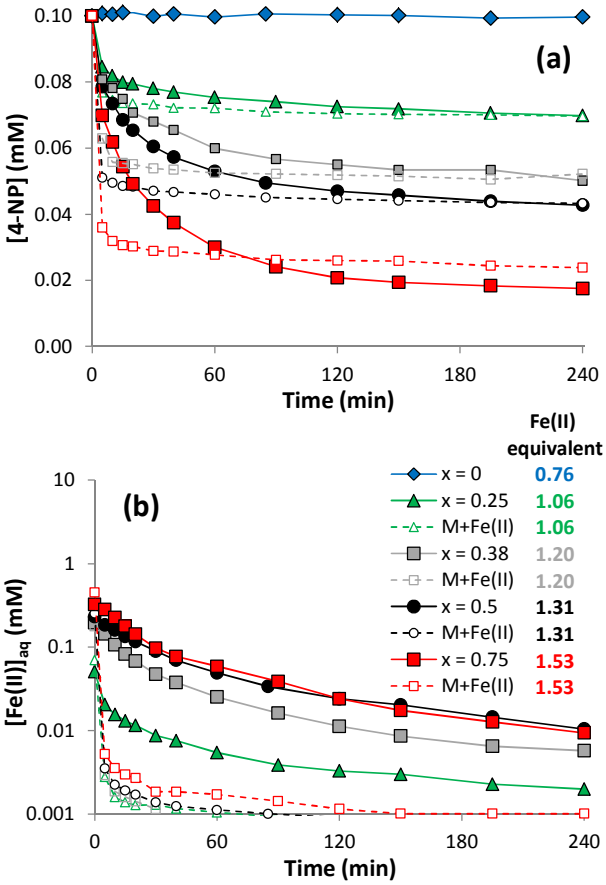
(a)
[4-NP] (mM)
0.10
0.08
0.06
0.04
0.02
0.00
0
60
120
180
240
Time (min)
(b)
[Fe(II)]aq (mM)
10
1
0.1
0.01
0.001
Time (min)
Fe(II) equivalent
x = 0 0.76
x = 0.25 1.06
M+Fe(II) 1.06
x = 0.38 1.20
M+Fe(II) 1.20
x = 0.5 1.31
M+Fe(II) 1.31
x = 0.75 1.53
M+Fe(II) 1.53

Figure 2

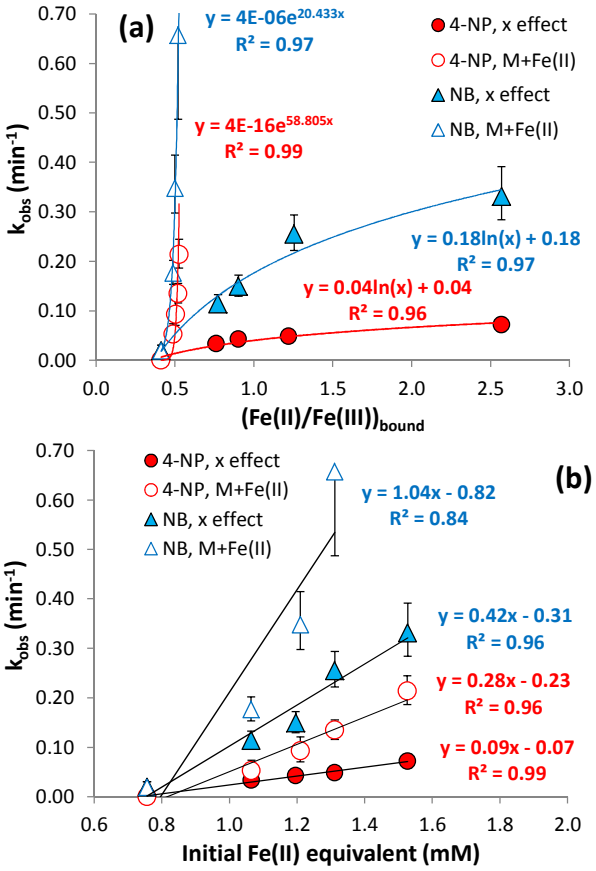
(a)
y = 4E-06e^20.433x
R² = 0.97
y = 4E-16e^58.805x
R² = 0.99
y = 0.18ln(x) + 0.18
R² = 0.97
y = 0.04ln(x) + 0.04
R² = 0.96
4-NP, x effect
4-NP, M+Fe(II)
NB, x effect
NB, M+Fe(II)
k_obs (min^-1)
(Fe(II)/Fe(III))_bound
(b)
y = 1.04x - 0.82
R² = 0.84
y = 0.42x - 0.31
R² = 0.96
y = 0.28x - 0.23
R² = 0.96
y = 0.09x - 0.07
R² = 0.99
Initial Fe(II) equivalent (mM)

Figure 3

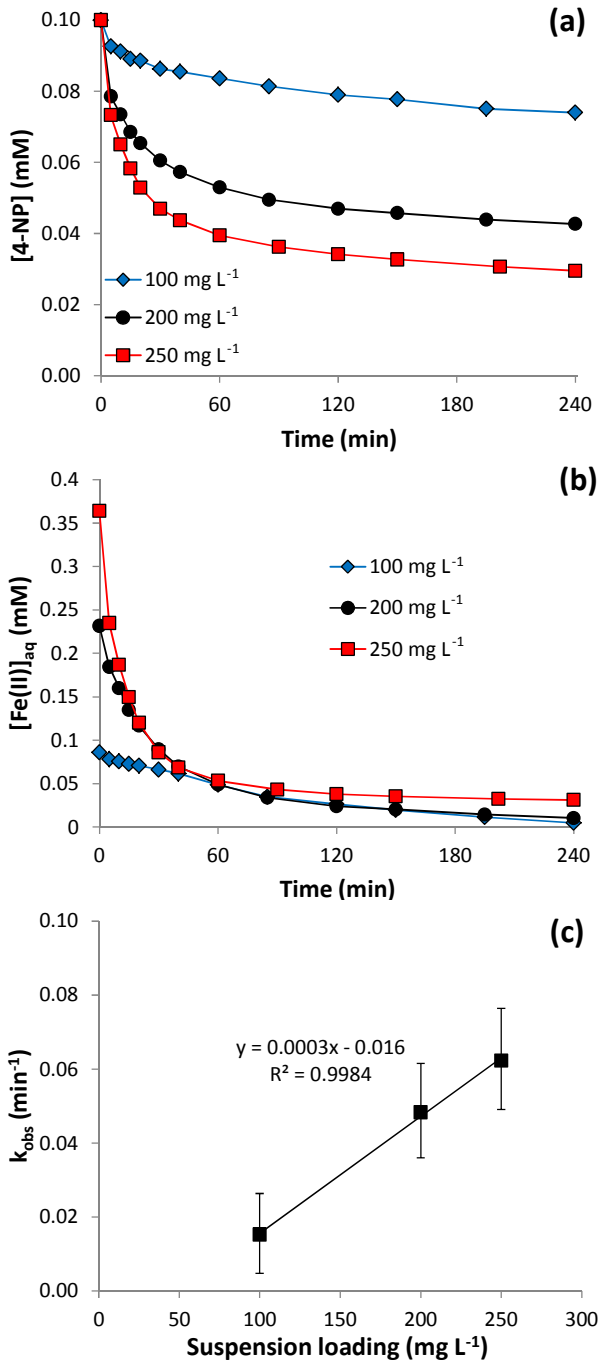
(a)
[4-NP] (mM)
0.10
0.08
0.06
0.04
0.02
0.00
100 mg L-1
200 mg L-1
250 mg L-1
0
60
120
180
240
Time (min)
(b)
[Fe(II)]aq (mM)
0.4
0.35
0.3
0.25
0.2
0.15
0.1
0.05
0
100 mg L-1
200 mg L-1
250 mg L-1
0
60
120
180
240
Time (min)
(c)
kobs (min-1)
0.10
0.08
0.06
0.04
0.02
0.00
y = 0.0003x - 0.016
R² = 0.9984
0
50
100
150
200
250
300
Suspension loading (mg L-1)

Figure 4

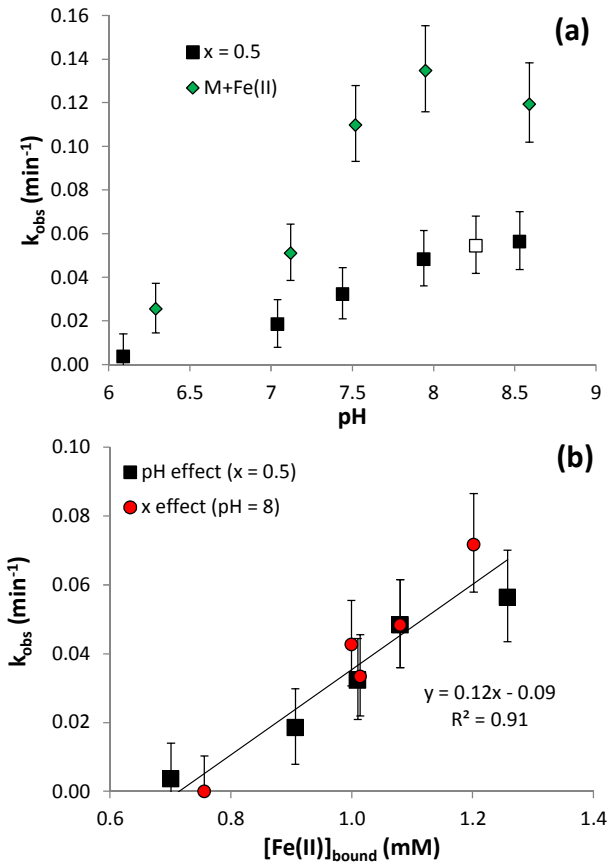
(a)
x = 0.5
M+Fe(II)
k_{obs} (min^{-1})
0.16
0.14
0.12
0.10
0.08
0.06
0.04
0.02
0.00
6
6.5
7
7.5
8
8.5
9
pH
(b)
pH effect (x = 0.5)
x effect (pH = 8)
k_{obs} (min^{-1})
0.10
0.08
0.06
0.04
0.02
0.00
y = 0.12x - 0.09
R² = 0.91
0.6
0.8
1.0
1.2
1.4
[Fe(II)]$_{bound}$ (mM)

TOC Graphic

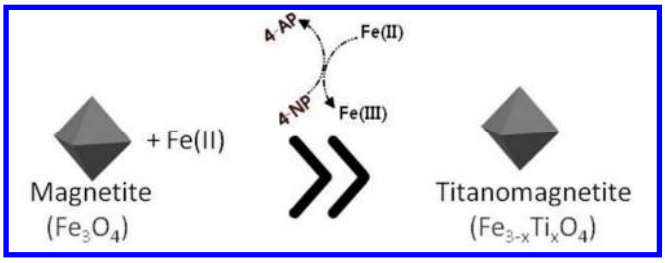
4-AP
Fe(II)
4-NP
Fe(III)
+ Fe(II)
Magnetite
(Fe_3O_4)
Titanomagnetite
($Fe_{3-x}Ti_xO_4$)